

# Hidden Markov Neural Networks

Lorenzo Rimella

ESOMAS, University of Torino and Collegio Carlo Alberto, Torino, IT

Nick Whiteley

School of Mathematics, University of Bristol, Bristol, UK

16th January 2025

## Abstract

We define an evolving in-time Bayesian neural network called a Hidden Markov Neural Network, which addresses the crucial challenge in time-series forecasting and continual learning: striking a balance between adapting to new data and appropriately forgetting outdated information. This is achieved by modelling the weights of a neural network as the hidden states of a Hidden Markov model, with the observed process defined by the available data. A filtering algorithm is employed to learn a variational approximation of the evolving-in-time posterior distribution over the weights. By leveraging a sequential variant of Bayes by Backprop, enriched with a stronger regularization technique called variational DropConnect, Hidden Markov Neural Networks achieve robust regularization and scalable inference. Experiments on MNIST, dynamic classification tasks, and next-frame forecasting in videos demonstrate that Hidden Markov Neural Networks provide strong predictive performance while enabling effective uncertainty quantification.

## 1 Introduction

Hidden Markov models (HMMs) are an efficient statistical tool for identifying patterns in dynamic datasets, with applications ranging from speech recognition (Rabiner and Juang, 1986) to computational biology (Krogh et al., 2001). Neural networks (NNs) are currently the most popular models in machine learning and artificial intelligence, demonstrating outstanding performance across several fields. In this paper, we propose a novel hybrid model called *Hidden Markov Neural Networks* (HMNNs), which combines Factorial Hidden Markov Models (Ghahramani and Jordan, 1997) and neural networks.

Intuitively, we aim to perform Bayesian inference on a time-evolving NN. However, computing the posterior distribution over the weights of even a static NN is a complex and generally intractable task. The extensive literature on variational Bayes (Blei et al., 2017) and its success in Bayesian inference for NNs (Graves, 2011; Kingma and Welling, 2013; Blundell et al., 2015) has motivated us to adopt this technique in HMNNs. In particular, the resulting procedure becomes the sequential counterpart of the Bayes by Backprop algorithm proposed by Blundell

et al. (2015). As in Blundell et al. (2015), the reparameterization trick (Kingma and Welling, 2013) plays a pivotal role in generating unbiased and low-variance estimates of the gradient.

HMNNs are particularly suited for time-series forecasting and continual learning (Wang et al., 2024). As noted by Kurle et al. (2019), much of the research in this area has focused on preventing forgetting (Kirkpatrick et al., 2017; Nguyen et al., 2017; Ritter et al., 2018). However, sudden changes in the statistical properties of the data may be an intrinsic feature of the generating process. In such cases, preserving all prior knowledge is not desirable, and it becomes necessary to forget irrelevant information. This can be achieved through the application of a Markov transition kernel (Kurle et al., 2019), which can be interpreted as the transition kernel of an HMM. In this sense, HMNNs adopt the adaptation idea proposed by Kurle et al. (2019) and extend it by leveraging the well-established framework of HMMs, further generalizing it to a broader class of variational approximations and stochastic kernels.

An alternative to variational Bayes is particle approximation via Sequential Monte Carlo (Chopin and Papaspiliopoulos, 2020). However, these algorithms are known to suffer from the curse of dimensionality (Rebeschini et al., 2015), making them unfeasible even for simple NN architectures.

## 2 Hidden Markov Neural Networks

For a time horizon  $T \in \mathbb{N}$ , a Hidden Markov model (HMM) is a bivariate process composed by an unobserved Markov chain  $(W_t)_{t=0,\dots,T}$ , called the hidden process, and a collection of observations  $(\mathcal{D}_t)_{t=1,\dots,T}$ , called the observed process, where the single observation at  $t$  is conditionally independent of all the other variables given the hidden process at the corresponding time step. We consider the case where the latent state-space is  $\mathbb{R}^V$ , with  $V$  finite set, and  $\mathcal{D}_t$  is valued in  $\mathbb{D}$  whose form is model specific (discrete,  $\mathbb{R}^d$  with  $d \in \mathbb{N}$ , etc.). To describe the evolution of an HMM three quantities are needed: the initial distribution, the transition kernel and the emission distribution. We use  $\lambda_0(\cdot)$  for the probability density function of  $W_0$  (initial distribution). We write  $p(W_t, \cdot | W_{t-1})$  for the conditional probability density function of  $W_t$  given  $W_{t-1}$  (transition kernel of the Markov chain). We call  $g(W_t, \mathcal{D}_t)$  the conditional probability mass or density function of  $\mathcal{D}_t$  given  $W_t$  (emission distribution).

We introduce a novel HMM called a Hidden Markov neural network (HMNN) where the hidden process describes the evolution of the weights of a neural network. For instance, in the case of feed-forward neural networks, the finite set  $V$  collects the location of each weight and  $v \in V$  can be thought of as a triplet  $(l, i, j)$  saying that the weight  $W_t^v$  is a weight of the NN at time  $t$ , and precisely related to the connection of the hidden unit  $i$  (or input feature  $i$  if  $l - 1 = 0$ ) in the layer  $l - 1$  with the hidden unit  $j$  in the layer  $l$  (which might be the output layer). In such a model we also assume that the weights evolve independently from each other, meaning that the transition kernel factorizes as follows:

$$p(W_{t-1}, W_t) = \prod_{v \in V} p^v(W_{t-1}^v, W_t^v), \quad W_{t-1}, W_t \in \mathbb{R}^V. \quad (1)$$

Under this assumption, an HMNN is a well-known class of HMM called Factorial Hidden Markov model (FHMM) (Ghahramani and Jordan, 1997), see Figure 1 for a graphical representation. Note that this factorization is key to ensure the computational cost of performing

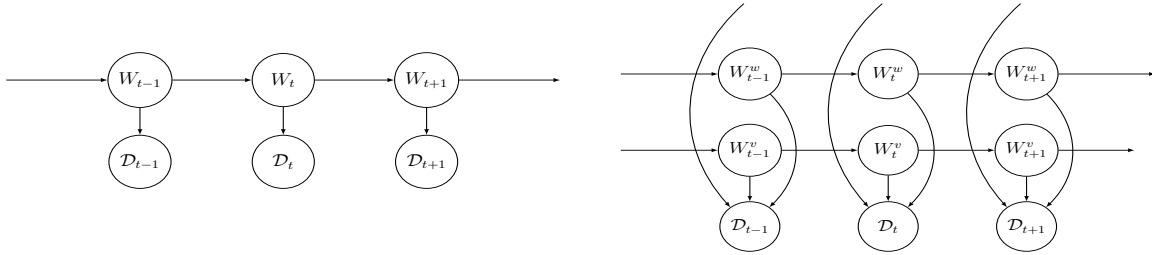


**Figure 1:** On the left: the conditional independence structure of an HMM. On the right: the conditional independence structure of an FHMM

inference does not blow up, and, in some scenarios, it allows to perform close-form calculations, see subsection 2.3. As an alternative one could use a block structure (Rebeschini et al., 2015), which requires, however, to keep track of the correlations within blocks.

There is no restriction on the form of the neural network or the data  $\mathcal{D}_t$ , however, we focus on a feed-forward neural network framework and on a supervised learning scenario where the observed process is composed by an input  $x_t$  and output  $y_t$ , such that the neural network associated to the weights  $W_t$  maps the input onto a probability distribution on the space of the output, which represents the emission distribution  $g(W_t, \mathcal{D}_t)$ .

## 2.1 Filtering algorithm for HMNN

The filtering problem aims to compute the conditional distributions of  $W_t$  given  $\mathcal{D}_1, \dots, \mathcal{D}_t$ , which is called filtering distribution. In this paper, we use the operator notation from Rebeschini et al. (2015), which gives us a way to compactly represent the filtering algorithm. We refer to Rebeschini et al. (2015); Chopin and Papaspiliopoulos (2020) for a thorough review.

We denote the filtering distribution with  $\pi_t$  and, ideally, we can compute it with a forward step through the data:

$$\pi_0 := \lambda_0, \quad \pi_t := C_t P \pi_{t-1}, \quad (2)$$

where  $P$ ,  $C_t$  are called prediction operator and correction operator and they are defined as follows:

$$P \pi_{t-1}(A) := \int \mathbb{I}_A(W_t) p(W_{t-1}, W_t) \pi_{t-1}(W_{t-1}) dW_{t-1} dW_t, \quad (3)$$

$$C_t \pi_t(A) := \frac{\int \mathbb{I}_A(W_t) g(W_t, \mathcal{D}_t) \pi_t(W_t) dW_t}{\int g(W_t, \mathcal{D}_t) \pi_t(W_t) dW_t}, \quad (4)$$

with  $\pi_{t-1}, \pi_t$  probability density functions,  $\mathbb{I}(\cdot)$  indicator function and  $A$  set in the sigma field of  $\mathbb{R}^V$ . Throughout the paper, we refer to our target distribution as the filtering distribution  $\pi_t$ , which is indeed the time-evolving posterior distribution over the weights of our NN. Recursion (2) is intractable for any non-linear architecture of the underlying neural network. As a solution, we can apply variational inference, which allows us to approximate a posterior distribution when operations cannot be performed in closed form. The use of variational inference is then crucial to allow us to use any activation function in our NN.

Variational inference can be used to approximate sequentially the target distribution  $\pi_t$  with a variational approximation  $q_{\theta_t}$  belonging to a pre-specified class of distributions  $\mathcal{Q}$ . The approximate distribution  $q_{\theta_t}$  is uniquely identified inside the class of distributions by a vector of parameters  $\theta_t$ , which is chosen to minimize a Kullback-Leibler (**KL**) divergence criteria:

$$q_{\theta_t} := \arg \min_{q_{\theta} \in \mathcal{Q}} \mathbf{KL}(q_{\theta} || \pi_t) = \arg \min_{q_{\theta} \in \mathcal{Q}} \mathbf{KL}(q_{\theta} || \mathbf{C}_t \mathbf{P} \pi_{t-1}), \quad (5)$$

where the Kullback-Leibler divergence can be rewritten as:

$$\mathbf{KL}(q_{\theta} || \mathbf{C}_t \mathbf{P} \pi_{t-1}) = \text{const.} + \mathbf{KL}(q_{\theta} || \mathbf{P} \pi_{t-1}) - \mathbb{E}_{q_{\theta}(w)} [\log (g(w, \mathcal{D}_t))], \quad (6)$$

because of the properties of the correction operator (4). From the above representation, we can also observe that minimizing the Kullback-Leibler divergence is equivalent to maximising the Evidence lower bound (**ELBO**):

$$\mathbf{ELBO}(q_{\theta}; \pi_{t-1}, \mathcal{D}_t) = \mathbb{E}_{q_{\theta}(w)} [\log (g(w, \mathcal{D}_t))] - \mathbf{KL}(q_{\theta} || \mathbf{P} \pi_{t-1}). \quad (7)$$

Sequential training using (5) is again intractable because it requires the filtering distribution at time  $t - 1$ , i.e.  $\pi_{t-1}$ . Although, under a good optimization, we could consider  $q_{\theta_t} \approx \pi_t$  when  $\pi_{t-1}$  is known, similarly  $q_{\theta_{t-1}} \approx \pi_{t-1}$  when  $\pi_{t-2}$  is known, and so on. Given that  $\pi_0$  is our prior knowledge  $\lambda_0$  on the weights before training, we can find a  $q_{\theta_1}$  that approximates  $\pi_1$  using (5) and then we can propagate forward our approximation by following the previous logic. In this way, an HMNN is trained sequentially on the same flavour of (5), by substituting the optimal filtering with the last variational approximation. As for the optimal procedure, we define an approximated filtering recursion, where  $\tilde{\pi}_t$  stands for the sequential variational approximation of  $\pi_t$ :

$$\tilde{\pi}_0 := \lambda_0, \quad \tilde{\pi}_t := \mathbf{V}_{\mathcal{Q}} \mathbf{C}_t \mathbf{P} \tilde{\pi}_{t-1}, \quad (8)$$

where the operators  $\mathbf{P}, \mathbf{C}_t$  are as in recursion (2) and the operator  $\mathbf{V}_{\mathcal{Q}}$  is defined as follows:

$$\mathbf{V}_{\mathcal{Q}} \rho := \arg \min_{q_{\theta} \in \mathcal{Q}} \mathbf{KL}(q_{\theta} || \rho), \quad (9)$$

with  $\rho$  being a probability distribution and  $\mathcal{Q}$  being the class of variational distributions, e.g. in (8) we have  $\rho = \mathbf{C}_t \mathbf{P} \tilde{\pi}_{t-1}$ . Note that, in this final notation, we are hiding the dependence on the variational parameters  $\theta$ .

Observe that this approach follows the assumed density filter paradigm (Sorenson and Stuberud, 1968; Minka, 2001), where the true posterior is projected onto a family of distributions which is easy to work with, and then propagated forward.

## 2.2 Sequential reparameterization trick

The minimization procedure exploited in recursion (8) cannot be solved in a closed form and we propose to find a suboptimal solution through gradient descent. Consider a general time step  $t$ , where we want to approximate  $\pi_t$  with  $\tilde{\pi}_t = q_{\theta_t}$ . This requires an estimate of the gradient of

$\text{KL}(q_\theta \| \mathbf{C}_t \mathbf{P} \tilde{\pi}_{t-1})$ . As explained in [Blundell et al. \(2015\)](#), if  $W \sim q_\theta$  can be rewritten as  $\epsilon \sim \nu$  through a deterministic transformation  $h$ , i.e.  $W = h(\theta, \epsilon)$ , then:

$$\begin{aligned} \frac{\partial \text{KL}(q_\theta \| \mathbf{C}_t \mathbf{P} \tilde{\pi}_{t-1})}{\partial \theta} &= \mathbb{E}_{\nu(\epsilon)} \left[ \frac{\partial \log(q_\theta(W))}{\partial W} \frac{\partial W}{\partial \theta} + \frac{\partial \log(q_\theta(W))}{\partial \theta} \right]_{W=h(\theta, \epsilon)} \\ &\quad - \mathbb{E}_{\nu(\epsilon)} \left[ \frac{\partial \log(\mathbf{P} \tilde{\pi}_{t-1}(W))}{\partial W} \frac{\partial W}{\partial \theta} \right]_{W=h(\theta, \epsilon)} \\ &\quad - \mathbb{E}_{\nu(\epsilon)} \left[ \frac{\partial \log(g(W, \mathcal{D}_t))}{\partial W} \frac{\partial W}{\partial \theta} \right]_{W=h(\theta, \epsilon)} \end{aligned} \quad (10)$$

where we used (6) to simplify the form of the equation (see supplementary material). Given (10) we can estimate the expectation  $\mathbb{E}_{\nu(\epsilon)}$  via straightforward Monte Carlo sampling:

$$\begin{aligned} \frac{\partial \text{KL}(q_\theta \| \mathbf{C}_t \mathbf{P} \tilde{\pi}_{t-1})}{\partial \theta} &\approx \frac{1}{N} \sum_{i=1}^N \left\{ \left[ \frac{\partial \log(q_\theta(W))}{\partial W} \frac{\partial W}{\partial \theta} + \frac{\partial \log(q_\theta(W))}{\partial \theta} \right]_{W=h(\theta, \epsilon)} \right. \\ &\quad \left. - \left[ \frac{\partial \log(\mathbf{P} \tilde{\pi}_{t-1}(W))}{\partial W} \frac{\partial W}{\partial \theta} \right]_{W=h(\theta, \epsilon)} \right. \\ &\quad \left. - \left[ \frac{\partial \log(g(W, \mathcal{D}_t))}{\partial W} \frac{\partial W}{\partial \theta} \right]_{W=h(\theta, \epsilon)} \right\}_{\epsilon=\epsilon^{(i)}} \end{aligned} \quad (11)$$

with  $\epsilon^{(i)} \sim \nu$  and  $N$  the size of the Monte Carlo sample. Given the Monte Carlo estimate of the gradient, we can then update the parameters  $\theta_t$ , related to the variational approximation at time  $t$ , according to any gradient descent technique. Algorithm 1 displays this procedure and, for the sake of simplicity, we write the algorithm with an update that follows a vanilla gradient descent.

---

**Algorithm 1** Approximate filtering recursion

---

*Set:*  $\tilde{\pi}_0 = \lambda_0$

**for**  $t = 1, \dots, T$  **do**

*Initialize:*  $\theta_t$

**repeat**

$\epsilon^{(i)} \sim \nu, \quad i = 1, \dots, N$

*Estimate the gradient*  $\nabla$  *with (11) evaluated in*  $\theta = \theta_t$

*Update the parameters:*  $\theta_t = \theta_t - l \nabla$

**until** *Maximum number of iterations*

*Set:*  $\tilde{\pi}_t = q_{\theta_t}$

**end for**

**Return:**  $(\theta_t)_{t=1, \dots, T}$

---

As suggested in the literature ([Graves, 2011](#); [Blundell et al., 2015](#)), the cost function in (6) is suitable for minibatches optimization. This might be useful when at each time step  $\mathcal{D}_t$  is made of multiple data and so a full computation of the gradient is computationally prohibitive.

### 2.3 Gaussian case

A fully Gaussian model, i.e. when both the transition kernel and the variational approximation are Gaussian distributions, is not only convenient because of the form of  $h(\theta, \epsilon)$  is trivial, but also because there exists a closed form solution for  $\mathbb{P}\tilde{\pi}_{t-1}$ . Another appealing aspect of the Gaussian choice is that similar results hold for the scale mixture of Gaussians, which allows us to use a more complex variational approximation and a transition kernel of the same form as the prior distribution in [Blundell et al. \(2015\)](#). Start by considering the variational approximation. We choose  $q_\theta := \bigotimes_{v \in V} q_\theta^v$  where  $q_\theta^v$  is a mixture of Gaussian with parameters  $\theta^v = (m^v, s^v)$  and  $\gamma^v$  hyperparameter. Precisely, for a given weight  $W^v$  of the feed-forward neural network:

$$q_\theta^v(W^v) := \gamma^v \mathcal{N}(W^v | m^v, (s^v)^2) + (1 - \gamma^v) \mathcal{N}(W^v | 0, (s^v)^2), \quad (12)$$

where  $\gamma^v \in (0, 1]$ ,  $m^v \in \mathbb{R}$ ,  $(s^v)^2 \in \mathbb{R}_+$ , and  $\mathcal{N}(\cdot | \mu, \sigma^2)$  is the Gaussian density with mean  $\mu$  and variance  $\sigma^2$ . We refer to this technique as variational DropConnect because it can be interpreted as setting around zero with probability  $1 - \gamma^v$  the weight in position  $v$  of the neural network and so it plays a role of regularization similar to [Wan et al. \(2013\)](#). Under variational DropConnect the deterministic transformation  $h(\theta, \epsilon)$  is still straightforward. Indeed, given that  $q_\theta$  factorises, then  $h(\theta, \epsilon) = (h^v(\theta^v, \epsilon^v))_{v \in V}$  (each  $W^v$  depends only on  $\theta^v$ ) and  $W^v$  is distributed as (12) which is equivalent to consider:

$$W^v = \eta^v m^v + \xi^v s^v, \quad \text{with } \eta^v \sim \text{Be}(\cdot | \gamma^v), \quad \xi^v \sim \mathcal{N}(\cdot | 0, 1), \quad (13)$$

where  $\text{Be}(\cdot | p)$  is the Bernoulli density with parameter  $p$ . Observe that the distribution of (13) is (12), as the  $\gamma^v$  is coming from the Bernoulli random variable  $\eta^v$ , which activates or not the mean  $m^v$ , while the  $\xi^v$  represents the Gaussian term. Hence  $h^v(\theta^v, \epsilon^v) = \eta^v m^v + \xi^v s^v$ , where  $\theta^v = (m^v, s^v)$  and  $\epsilon^v = (\eta^v, \xi^v)$  with  $\eta^v$  Bernoulli with parameter  $\gamma^v$  and  $\xi^v$  standard Gaussian, meaning that we just need to sample from a Bernoulli and a Gaussian distribution independently. The collection of hyperparameters  $(\gamma^v)_{v \in V}$  represents the variational DropConnect rate per each weight in the NN and we generally choose  $\gamma^v = \gamma \in (0, 1]$  per each  $v \in V$ , i.e. we have a global regularization parameter. Remark that  $(\gamma^v)_{v \in V}$  must be considered as fixed and cannot be learned during training, because from (10) we need the distribution of  $\epsilon$  to not be dependent on the learnable parameters. Consider now the transition kernel. It is chosen to be a scale mixture of Gaussians with parameters  $\phi, \alpha, \sigma, c, \mu$ :

$$p(W_{t-1}, W_t) := \phi \mathcal{N}(W_t | \mu + \alpha(W_{t-1} - \mu), \sigma^2 \mathbf{I}_V) + (1 - \phi) \mathcal{N}(W_t | \mu + \alpha(W_{t-1} - \mu), (\sigma^2/c^2) \mathbf{I}_V), \quad (14)$$

where  $\phi \in [0, 1]$ ,  $\mu \in \mathbb{R}^V$ ,  $\alpha \in [0, 1)$ ,  $\sigma \in \mathbb{R}_+$ ,  $\mathbf{I}_V$  is the identity matrix on  $\mathbb{R}^{V,V}$ ,  $c \in \mathbb{R}_+$  and  $c > 1$ . Intuitively, the transition kernel tells us how we are expecting the weights to be in the next time step given the states of the weights at the current time. We can interpret it, along with the previous variational approximation, as playing the role of an evolving prior distribution which constrains the new posterior distribution in regions that are determined from the previous training step. The choice of the transition kernel is crucial. A too conservative kernel would constrain too much training and the algorithm would not be able to learn patterns in new data. On the contrary, a too flexible kernel could just forget what was learned previously and adapt to the new data only.

Notation	Meaning
$W_t, \mathcal{D}_t$	hidden weights of an NN and observed data at time $t$
$p(W_{t-1}, W_t)$	Markov transition kernel of the weights of the NN
$g(W_t, \mathcal{D}_t)$	probability distribution of the data given the weights
$v$	a weight of the NN, it is also used to represent marginal quantities
$\pi_t, \tilde{\pi}_t$	filtering distribution and its approximation at time $t$
$P, C_t$	prediction operator and correction operator at time $t$
$V_{\mathcal{Q}}$	operator that minimize the KL-divergence on the class $\mathcal{Q}$
$q_{\theta}, \theta$	variational approximation and its parameters
$h(\theta, \cdot)$	transformation function in the reparameterization trick
$\gamma^v$	scale mixture of Gaussians probability of weight $v$
$m_t^v$	scale mixture of Gaussians mean of weight $v$ at time $t$
$s_t^v$	scale mixture of Gaussians standard dev. of weight $v$ at time $t$
$\phi$	scale mixture of Gaussians probability of transition kernel
$\mu$	scale mixture of Gaussians stationary mean of transition kernel
$\alpha$	scale mixture of Gaussians mean scaling of transition kernel
$\sigma$	scale mixture of Gaussians big-jump standard dev. of transition kernel
$\sigma/c$	scale mixture of Gaussians small-jump standard dev. of transition kernel

**Table 1:** Notation summary.

As we are considering Gaussian distribution we can solve  $P\tilde{\pi}_{t-1}$  in closed form, and, precisely, we get another scaled mixture of Gaussian distributions. We can then directly work on the Gaussian density  $P\tilde{\pi}_{t-1}(W_{t-1})$ , which is a product over  $v \in V$  of scaled mixture of Gaussian densities. Specifically, consider a general weight  $v \in V$  and call  $(P\tilde{\pi}_{t-1})^v(W_{t-1}^v)$  the marginal density of  $P\tilde{\pi}_{t-1}$  on the component  $v$ . If  $m_{t-1}^v, s_{t-1}^v$  are the estimates of  $m^v, s^v$  at time  $t-1$  then:

$$\begin{aligned}
(P\tilde{\pi}_{t-1})^v(W_{t-1}^v) = & \gamma^v \phi \mathcal{N}(W_{t-1}^v | \mu^v - \alpha(\mu^v - m_{t-1}^v), \sigma^2 + \alpha^2(s_{t-1}^v)^2) \\
& + (1 - \gamma^v) \phi \mathcal{N}(W_{t-1}^v | \mu^v - \alpha\mu^v, \sigma^2 + \alpha^2(s_{t-1}^v)^2) \\
& + \gamma^v(1 - \phi) \mathcal{N}(W_{t-1}^v | \mu^v - \alpha(\mu^v - m_{t-1}^v), \sigma^2/c^2 + \alpha^2(s_{t-1}^v)^2) \\
& + (1 - \gamma^v)(1 - \phi) \mathcal{N}(W_{t-1}^v | \mu^v - \alpha\mu^v, \sigma^2/c^2 + \alpha^2(s_{t-1}^v)^2).
\end{aligned} \tag{15}$$

We can observe that (15) is again a scale mixture of Gaussians, where all the variances are influenced by the variances at the previous time step according to  $\alpha^2$ . On the one hand, the variational DropConnect rate  $\gamma^v$  tells how to scale the mean of the Gaussians according to the previous estimates  $m_{t-1}^v$ . On the other hand,  $\phi$  controls the entity of the jumps by allowing the weights to stay in place with a small variance  $\sigma^2/c^2$  and permitting big jumps with  $\sigma^2$  if necessary. As in [Blundell et al. \(2015\)](#), when learning  $s_t$  we use the transformation  $\tilde{s}_t$  such that  $s_t = \log(1 + \exp(\tilde{s}_t))$ .

Across section 2 we have declared multiple quantities which we summarize in Table 1.

## 2.4 Performance and uncertainty quantification

After running Algorithm 1, we obtain a sequence of variational approximations  $\tilde{\pi}_t = q_{\theta_t}$  for our filtering distributions  $\pi_t$ . These approximations represent the posterior distribution of  $W_t$ , meaning that we are approximating the distribution of  $W_t | \mathcal{D}_1, \dots, \mathcal{D}_t$  with a known distribution. Given a realization of  $W_t$ , we can compute  $g(W_t, \cdot)$ , which represents the likelihood at time  $t$  or, equivalently, the performance of the neural network (NN) with weights  $W_t$ . We generally assume the ability to compute the mean of  $\tilde{\pi}_t = q_{\theta_t}$ , i.e. the posterior mean, and to sample from it, i.e., obtain posterior samples. These two components allow us to assess the performance of our HMNN over time and evaluate how certain we are about that performance.

In our experiments, we typically refer to performance when evaluating our time-evolving NN using the posterior mean,  $\mathbb{E}_{\tilde{\pi}_t(W_t)}[W_t]$ . Conversely, when assessing uncertainty, we consider posterior samples,  $W_t^{(1)}, \dots, W_t^{(N)}$ .

## 3 Related Work

**Combining NNs and HMMs** Multiple attempts have been made in the literature to combine HMM and NN. In Franzini et al. (1990) an NN is trained to approximate the emission distribution of an HMM. Bengio et al. (1990) and Bengio et al. (1991) preprocess the data with an NN and then use the output as the observed process of a discrete HMM. Krogh and Riis (1999) propose *Hidden neural networks* where NNs are used to parameterize Class HMM, an HMM with a distribution over classes assigned to each state. Other recent works include: Johnson et al. (2016); Karl et al. (2016); Krishnan et al. (2017). In neuroscience, Aitchison et al. (2014) explores the idea of updating measures of uncertainty over the weights in a mathematical model of a neuronal network as part of a "Bayesian Plasticity" hypothesis of how synapses take uncertainty into account during learning. However, they did not focus on artificial neural networks and the computational challenges of using them for data analysis when network weights are statistically modelled as being time-varying.

**Bayesian DropConnect & DropOut** DropConnect (Wan et al., 2013; Mobiny et al., 2021) and DropOut (Srivastava et al., 2014; Salehin and Kang, 2023) are well-known techniques to prevent NN from overfitting. Kingma et al. (2015) proposes variational DropOut where they combined fully factorized Gaussian variational approximation with the local reparameterization trick to re-interpret DropOut with continuous noise as a variational method. Gal and Ghahramani (2016) extensively treat the connections between DropOut and Gaussian processes, and they show how to train NNs with DropOut (or DropConnect (Mobiny et al., 2019)) in a variational Bayes setting. Our version of variational DropConnect has several common aspects with the cited works, but the novelty resides in the regularization being induced by the variational approximation's choice and the corresponding reformulation of the reparameterization trick.

**Bayesian filtering** There are multiple examples of NN training through Bayesian filtering (Puskorius and Feldkamp, 1991, 1994, 2001; Shah et al., 1992; Feldkamp et al., 2003; Olivier et al., 2018). In particular, the recent work of Aitchison (2018) proposed AdaBayes and



AdaBayes-SS where updates resembling the Kalman filter are employed to model the conditional posterior distribution over a weight of an NN given the states of all the other weights. However, the main difference with HMNN is the dynamical evolution of the underlined NN, indeed Bayesian filtering methods do not consider any change in time.

**Continual learning** There are significant similarities between our work and continual learning methods. Here we do a quick overview of the most popular ones and we refer to Wang et al. (2024) for a complete review. Elastic Weight Consolidation (EWC) (Kirkpatrick et al., 2017) uses an L2-regularization that guarantees the weights of the NN for the new task being in the proximity of the ones from the old task. Variational continual learning (VCL) (Nguyen et al., 2017) learns a posterior distribution over the weights of an NN by approximating sequentially the true posterior distribution through variational Bayes and by propagating forward the previous variational approximation without (this is like setting our transition kernel to a Dirac delta). Online Laplace approximation (Ritter et al., 2018; Liu et al., 2023) proposes a recursive update for the parameters of a Gaussian variational approximation which involves Hessian of the newest negative log-likelihood. None of the cited techniques builds dynamic models, and even if this could be solved by storing the weights at each training step there is no forgetting, meaning that EWC, VCL, and Online Laplace focus on overcoming catastrophic forgetting and they are not able to avoid outdated information. Lastly, the most similar procedure to HMNNs is the one proposed by Kurle et al. (2019), where the authors perform model adaption with Bayes forgetting through the application of a stochastic kernel. However, HMMs are not even cited and the form of the kernel and variational approximation are restricted to Gaussian distributions, not mixtures.

## 4 Experiments

In this section, we test the performance of HMNNs. Similar to Blundell et al. (2015), we focus our study on simple feed-forward neural networks, leaving the exploration of more complex architectures for future work. Notably, in our experiments, the computational cost per time step is comparable to that of Bayes by Backprop.

Firstly, we empirically demonstrate that variational DropConnect, i.e. using (12) as a variational approximation, yields better performance than Bayes by Backprop (Blundell et al., 2015) on MNIST (LeCun et al., 1998). Secondly, we provide an experiment to show how HMNNs work and how they can quantify uncertainty in a simple time-evolving classification setting built from the “two-moons” dataset (Pedregosa et al., 2011). We then highlight the ability of HMNNs to retrieve the evolution of true parameters in a conceptual drift scenario (Kurle et al., 2019). Specifically, we demonstrate that employing more complex variational approximations, compared to those used in Kurle et al. (2019), does not affect the retrieval process. Following this, we explore a more complex conceptual drift framework constructed from the MNIST dataset, comparing HMNNs to continual learning baselines (Kirkpatrick et al., 2017; Nguyen et al., 2017; Kurle et al., 2019). Finally, we show that HMNNs can also be applied to one-step-ahead forecasting in time-series. Specifically, we address a next-frame prediction task in the dynamic video texture of a waving flag (Chan and Vasconcelos, 2007; Boots et al., 2008; Basharat and Shah, 2009). Additional experimental details are provided in

the supplementary material.

The experiments are run on three different clusters: BlueCrystal Phase 4 (University of Bristol), Cirrus (one of the EPSRC Tier-2 National HPC Facilities) and The Cambridge Service for Data Driven Discovery (CSD3) (University of Cambridge).

## 4.1 Variational DropConnect

The experiment aims to understand if using a Gaussian mixture as a variational approximation can help improve Bayes by Backprop. We train on the MNIST dataset with the same setup of [Blundell et al. \(2015\)](#). We consider a small architecture with the vectorized image as input, two hidden layers with 400 rectified linear units ([Nair and Hinton, 2010](#); [Glorot et al., 2011](#)) and a softmax layer on 10 classes as output. We consider a fully Gaussian HMNN, as in subsection 2.3, with  $T = 1$ ,  $\alpha = 0$  and  $\mu = \mathbf{0}$  (kernel parameter), with  $\mathbf{0}$  being the zero vector. Note that such HMNN coincides with a single Bayesian neural network, meaning that we are simply training with Bayes by Backprop with the addition of variational DropConnect, see the supplementary material for more details. We train on about 50 combinations of the parameters  $(\gamma^v, \phi, \sigma, c)$  and learning rate, which are randomly extracted from pre-specified grids.

Model selection is done according to a validation score on a held-out validation set. We cluster the 50 combinations of the parameters by their values of  $\gamma^v$  and we report in Figure 2 the performance of the three best models per each  $\gamma^v$  value on the held-out validation set.

We then select the best models per each  $\gamma^v$  and we compute the performance on a held-out test set, see Table 2. We find out that values of  $\gamma^v < 1$  lead to better performance, motivating the use of variational DropConnect as a regularization technique.

**Table 2:** Classification accuracy (the bigger is the better) of best runs for MNIST on a held-out test set (MNIST test set).  $\gamma^v = 1$  refers to the case of Bayes by Backprop without variational DropConnect.

Parameter value	Accuracy
$\gamma^v = 0.25$	0.9838
$\gamma^v = 0.5$	0.9827
$\gamma^v = 0.75$	0.9825
$\gamma^v = 1$ ( <a href="#">Blundell et al., 2015</a> )	0.9814

## 4.2 Illustration: Two moons dataset

In this subsection, we provide an illustration of HMNN on the “two moons” dataset from “scikit-learn” ([Pedregosa et al., 2011](#)). This synthetic dataset produces two half circles in the plane which are binary classified. To create a time dimension we sequentially rotated these half circles. Specifically, over  $t = 0, 1, 2, 3, 4$  we generate new data from the “two moons” dataset and then apply a rotation with an increasing angle by keeping the label as simulated. We also consider two scenarios: one where the “two moons” are well separated, and another where the “two moons” are overlapping, see Figure 3.

Given the two training sets, a fully Gaussian HMNN is run for a fixed set of hyperparameters, see the supplementary material. For the neural network architecture we consider a bidimensional vector as input, i.e.  $(x, y)$  location, two hidden layers with 50 rectified linear

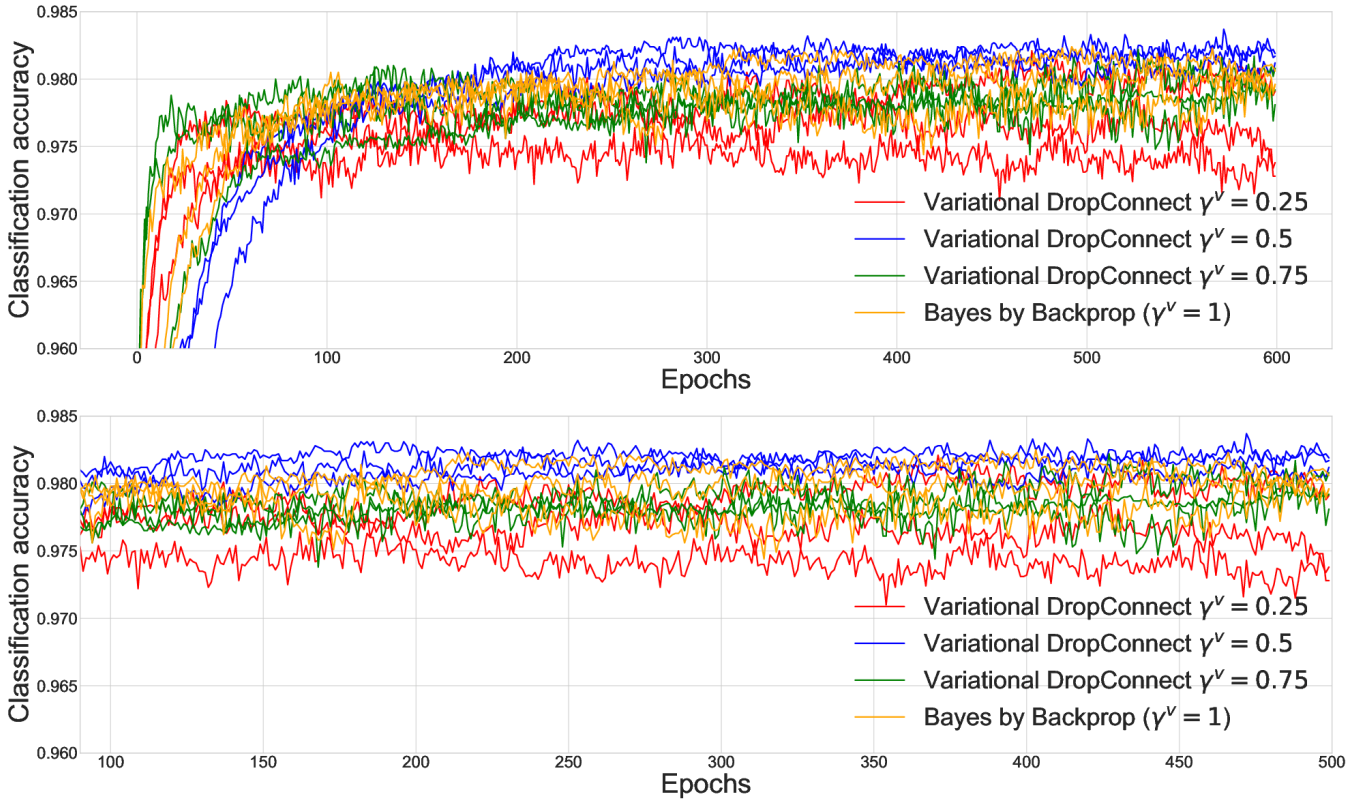


**Figure 2:** Performance on a validation set of a Bayes by Backprop with and without variational Drop-Connect. The plot on the bottom is a zoom-in of the plot on the top.

units, and a softmax layer on 2 classes as output. The result is an evolving in-time Bayesian neural network that is able to associate to each location on the plane a probability of being in one class or the other, and also to quantify uncertainty on these probabilities. Note that it is enough to report one of the two probabilities as the other one is the complement.

We illustrate these results in Figure 5, where the 95% credible interval is obtained via Monte Carlo sampling on the weights of the HMNN, see subsection 2.4. Here we can observe that the scenario with overlapping moon shows smoother transition between the two classification regions, meaning that we do not know which label to guess. In terms of uncertainty in the overlapping example, we are generally less confident about our probability estimates compared to the well-separated one. Moreover, in the well-separated example, there are some blank regions between two moons where the HMNN is completely uncertain about what to guess.

This can be further checked by plotting the length of the credible interval, see Figure 4. We can observe that where the two classes overlap the HMNN becomes less certain (bigger length of the credible interval) but it becomes completely uncertain (length close to one) in the region between the two moons and where no data are observed. Intuitively, with the yellow region in Figure 4 the HMNN is telling us: “I do not know”. We remark that this is one of the most important features of the Bayesian approach, which allows the model to be uncertain about the prediction and warn the user beforehand.

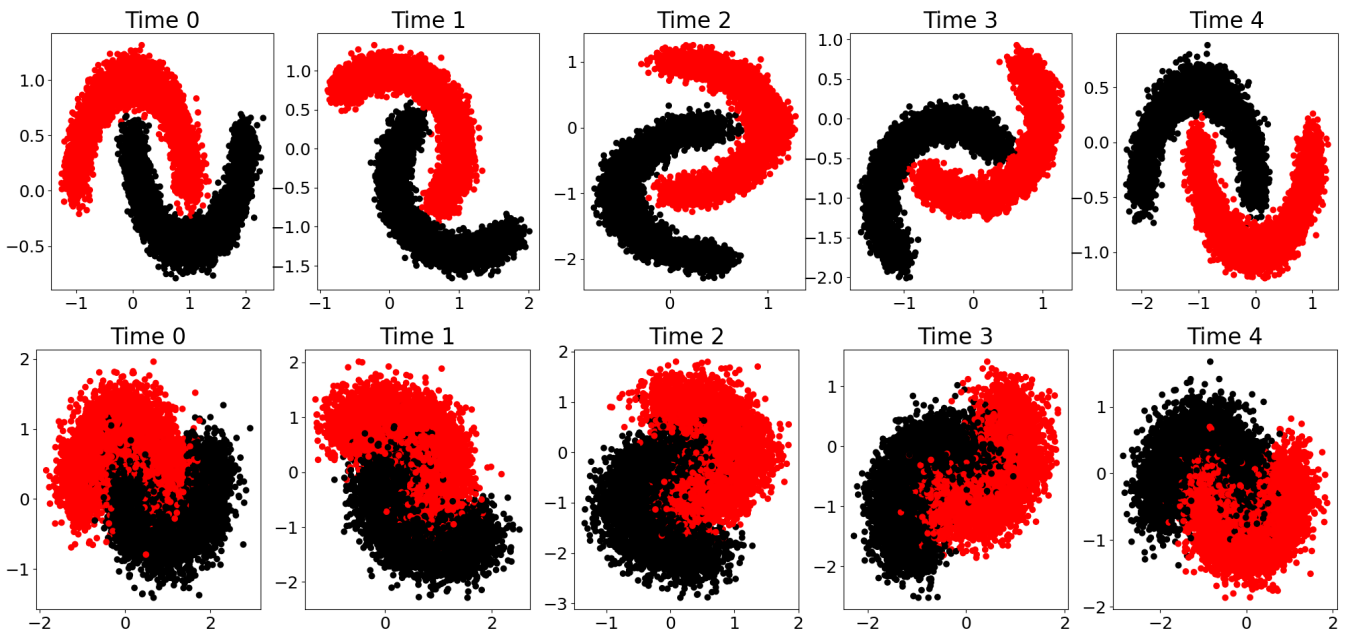


**Figure 3:** First row, well separated “two moons”. Second row, overlapping “two moons”. Different columns are associated with different time steps. Different colours are associated with different labels.

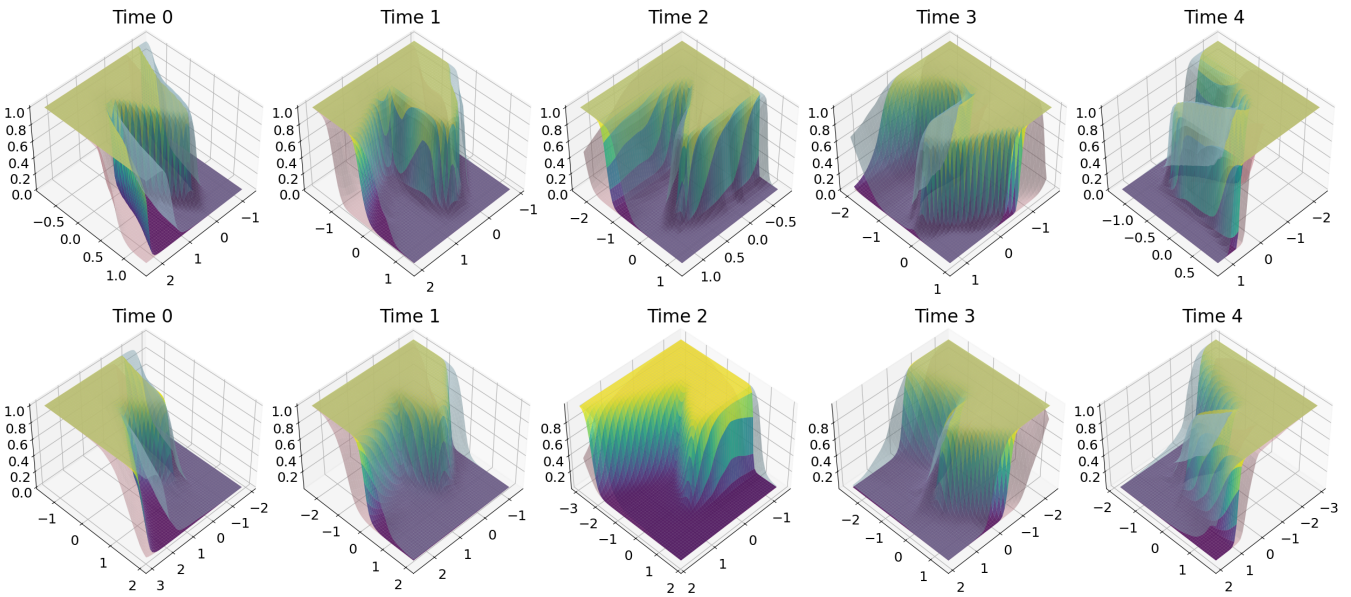


**Figure 4:** First row, well separated “two moons”. Second row, overlapping “two moons”. Different columns are associated with different time steps. The plot shows the length of the 95% credible interval. The blue and yellow surface is the probability prediction on the second class. Different coloured dots are associated with different labels.

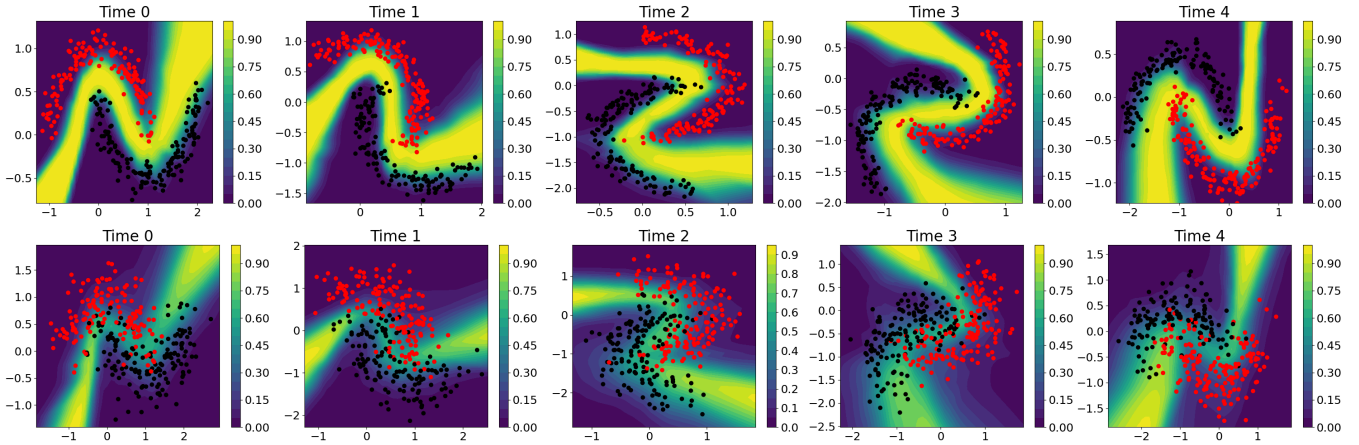


**Figure 5:** First row, well separated “two moons”. Second row, overlapping “two moons”. Different columns are associated with different time steps. The blue and yellow surface is the probability prediction on the second class. Pink and grey shaded surfaces represent the 95% credible intervals.

### 4.3 Concept drift: Logistic regression

In this subsection, we compare HMNN and the adaption with the Ornstein-Uhlenbeck process proposed by Kurle et al. (2019) on concept drift. As in Kurle et al. (2019) we consider a 2-dimensional logistic regression problem where the weights evolve in time:  $w_t^{(1)} = 10 \sin(at)$  and  $w_t^{(2)} = 10 \cos(at)$ , where  $a = 5\text{deg}/\text{sec}$  and  $t = 1, \dots, 700$ . Precisely, per each time step the data are generated in the following manner:

$$x_t^{(i)} \sim U(\cdot | -3, 3), \quad y_t^{(i)} \sim \text{Be} \left( \cdot \mid \text{sigmoid} \left( x_t^{(i)}, w_t \right) \right), \quad (16)$$

where  $U(\cdot | a, b)$  is the uniform distribution over the interval  $[a, b]$ ,  $i = 1, \dots, 10000$  with 10000 being the batch size per time step,  $w_t = (w_t^{(1)}, w_t^{(2)})$  and  $\text{sigmoid} \left( x_t^{(i)}, w_t \right)$  being the sigmoid function with weights  $w_t$  and input  $x_t^{(i)}$ .

Given the training set, a fully Gaussian HMNN is run under multiple combinations of hyperparameters. The experiments showed recovery of the oscillating nature of the weights in each combination. Figure 6 reports the results of one of the considered hyperparameters’ combinations and the findings from Kurle et al. (2019). We can conclude that HMNN is able, as for Kurle et al. (2019), to recover the sinusoidal curve of the true parameters even if the form of the posterior distribution approximation in HMNN is chosen to be a mixture of Gaussians. Remark that the aim of this section was not classification accuracy but rather the recovery of the oscillating nature of the weights.

### 4.4 Concept drift: Evolving classifier on MNIST

In this subsection, we compare HMNNs with continual learning baselines when the data-generating distribution is dynamic. We decide to artificially generate such a dataset from MNIST with the following procedure.

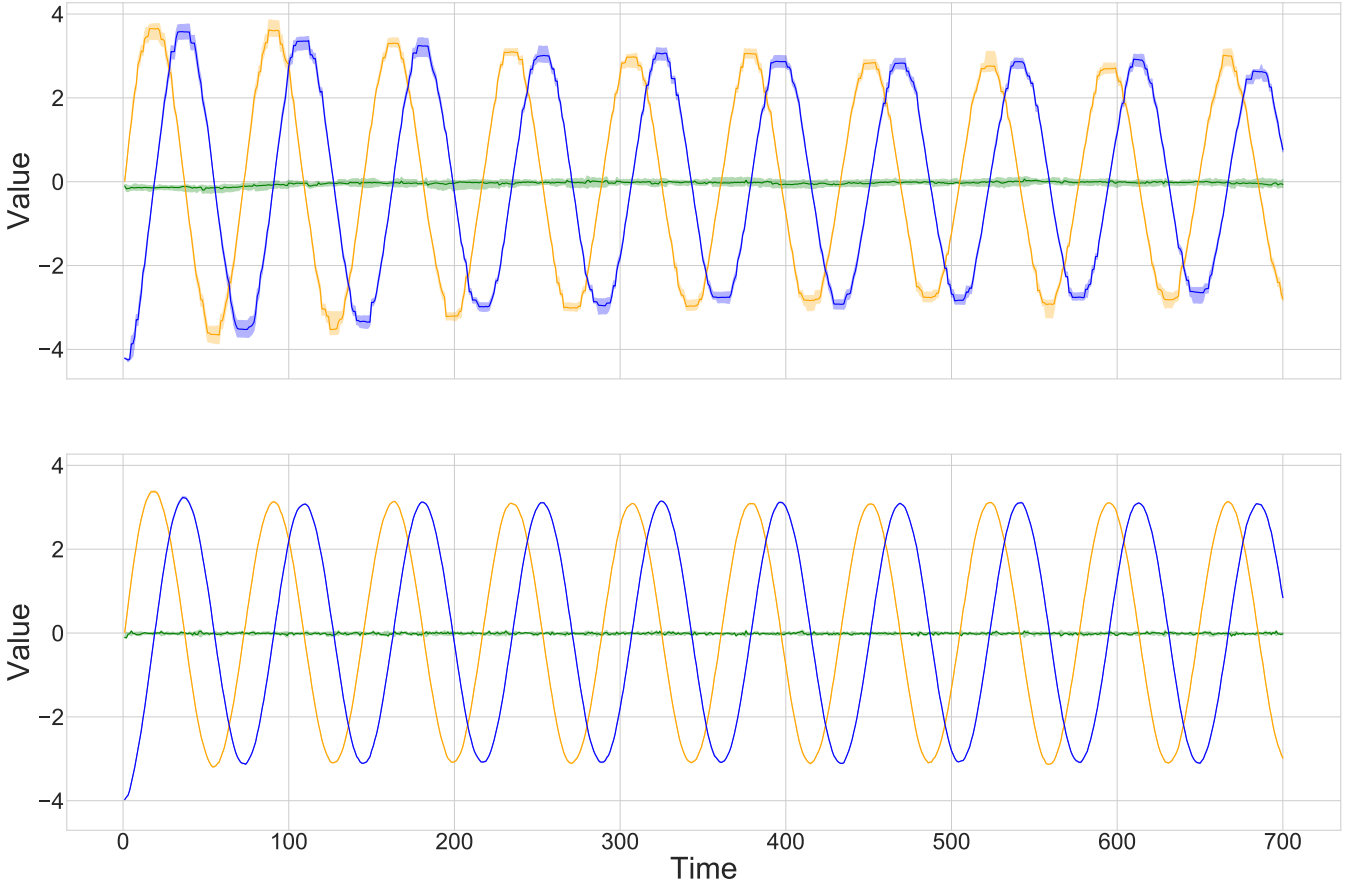


**Figure 6:** Mean of the approximate posterior distributions over 700 steps, credible intervals are built from multiple runs. Orange stands for  $w_t^{(1)}$ , blue stands for  $w_t^{(2)}$  and green is used for the bias. On the top, HMNN. On the bottom, adaption with Ornstein-Uhlenbeck process by [Kurle et al. \(2019\)](#).

1. We define two labellers:  $\mathcal{C}_1$ , naming each digit with its label in MNIST;  $\mathcal{C}_2$ , labelling each digit with its MNIST's label shifted by one unit, i.e. 0 is classified as 1, 1 is classified as 2,  $\dots$ , 9 is classified as 0.
2. We consider 19 time steps where each time step  $t$  is associated with a probability  $f_t \in [0, 1]$  and a portion of the MNIST's dataset  $\mathcal{D}_t$ .
3. At each time step  $t$  we randomly label each digit in  $\mathcal{D}_t$  with either  $\mathcal{C}_1$  or  $\mathcal{C}_2$  according to the probabilities  $f_t, 1 - f_t$ .

The resulting  $(\mathcal{D}_t)_{t=1, \dots, 19}$  is a collection of images where the labels evolve in  $t$  by switching randomly from  $\mathcal{C}_1$  to  $\mathcal{C}_2$  and vice-versa. Validation and test sets are built similarly. In such a scenario, we would ideally want to be able to predict the correct labels by learning sequentially a classifier that is capable of inferring part of the information from the previous time step and forgetting the outdated one. Remark that when  $f_t = 0.5$  the best we can do is a classification accuracy of 0.5 because  $\mathcal{C}_1$  and  $\mathcal{C}_2$  are indistinguishable.

We consider a fully Gaussian HMNN with  $\mu = m_{t-1}$  (kernel parameter), to encourage a

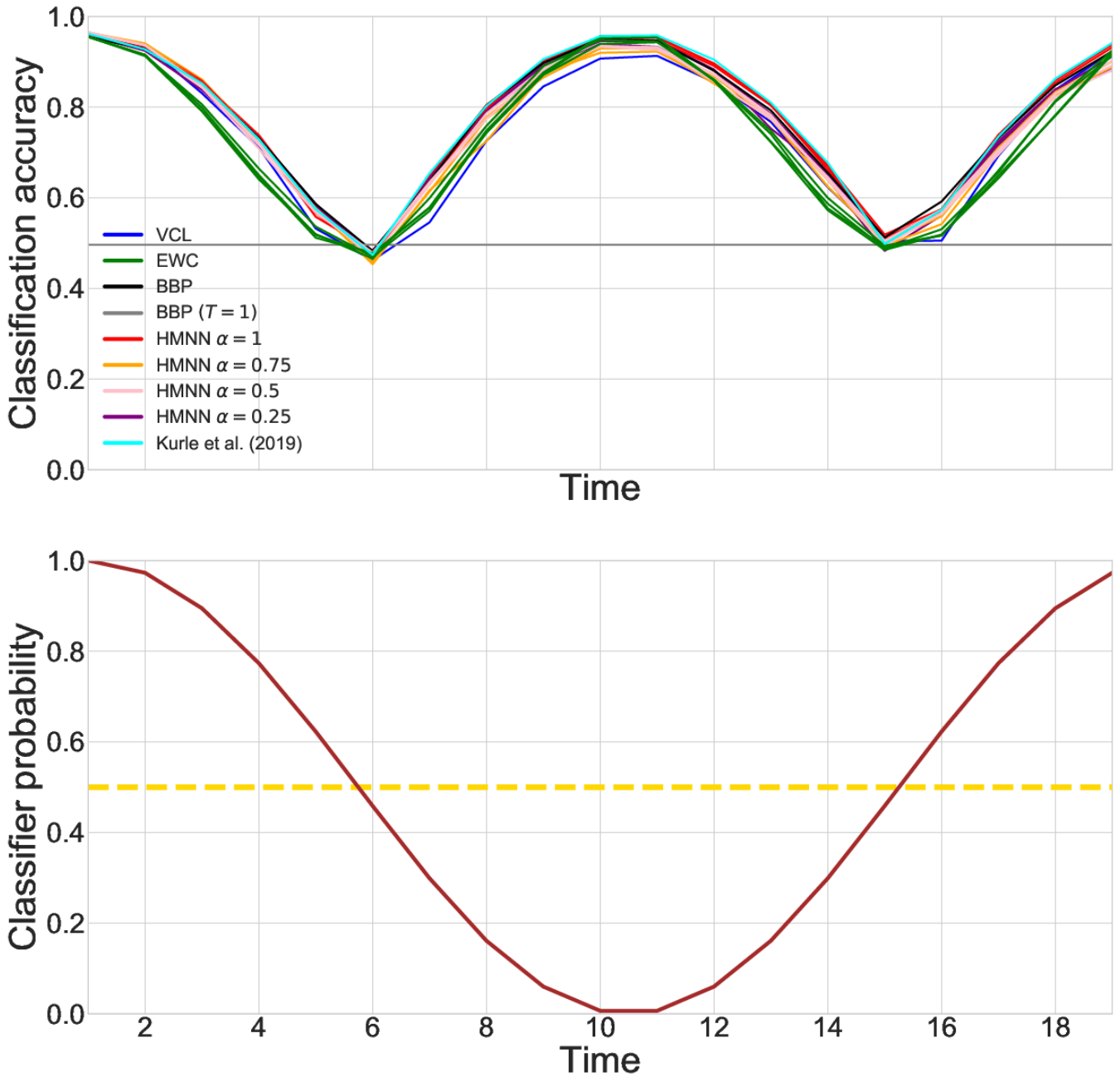


**Figure 7:** On the top, performances on a held-out validation set over time of evolving classifiers obtained with different algorithms. BBP refers to Bayes by Backprop trained sequentially. BBP ( $T=1$ ) refers to the training of Bayes by Backprop on the whole dataset. On the bottom, in brown evolution in time of the probability  $f_t$  of choosing the labeller  $\mathcal{C}_1$ ; in yellow the value 0.5.

strong memory of the past. The evolving in-time NN is composed of the vectorized image as input, two hidden layers with 100 rectified linear units and a softmax layer on 10 classes

as output. The parameters  $\alpha, \gamma^v$  are selected through the validation set while the other parameters are fixed before training. Along with the previous HMNN, we train sequentially five additional models for comparison: Variational continual learning (VCL), without coreset; Elastic weight consolidation (EWC), with tuning parameter chosen with the validation set; Bayes by Backprop trained sequentially on the dataset; Bayes by Backprop on the full dataset; Kurle et al. adaption with Ornstein-Uhlenbeck process (Kurle et al., 2019). Selected graphical performances on the validation sets are displayed in Figure 7.

To test the method we report the mean over time of the classification accuracy, which can be found in Table 3. For HMNN, Kurle et al., Bayes by Backprop, EWC and VCL we choose the parameters that perform the best on validation. We find that HMNN, the model by Kurle et al. (2019) and a sequential training of Bayes by Backprop perform the best. It is not surprising that continual learning methods fall behind. Indeed, EWC and VCL are built to preserve knowledge on the previous tasks, which might mix up  $\mathcal{C}_1$  and  $\mathcal{C}_2$  and confuse the network.

**Table 3:** Classification accuracy on a held-out test set for the evolving classifier (the bigger is the better). BBP refers to Bayes by Backprop trained sequentially. BBP (T=1) refers to the training of Bayes by Backprop on the whole dataset.

Model	Accuracy
BBP (T=1)	0.503
VCL	0.744
EWC	0.760
BBP	0.780
Kurle et al. (Kurle et al., 2019)	0.784
HMNN	0.786

## 4.5 One-step-ahead prediction for flag waving

We conclude by testing HMNNs on predicting the next frame in a video. The dataset is a sequence of images extracted from a video of a waving flag (Basharat and Shah, 2009; Venkatraman et al., 2015). The idea is to create an HMNN where the neural network at time  $t$  can predict the next frame, i.e. the NN maps frame  $t$  in frame  $t + 1$ . To measure the performance we use the metric suggested in Venkatraman et al. (2015) which is a standardized version of the RMSE on a chosen test trajectory:

$$\mathcal{M}(y_{1:T}, \hat{y}_{1:T}) := \sqrt{\frac{\sum_{t=1}^T \|y_t - \hat{y}_t\|_2^2}{\sum_{t=1}^T \|y_t\|_2^2}}, \quad (17)$$

where  $y_{1:T}$  is the ground truth on frames  $1, \dots, T$  and  $\hat{y}_{1:T}$  are the predicted frames. Unless specified differently,  $\hat{y}_{1:T}$  is a sequence of one-step-ahead predictions. To have a proper learning procedure we need multiple frames per time step, otherwise, the neural network would just learn the current frame. To overcome this problem we create a sliding window with 36 frames, meaning that at time step  $t$  we train on predicting frames  $t - 35, \dots, t$  from frames  $t - 36, \dots, t - 1$ , with  $t > 36$ . The choice of the length for the sliding window is empirical, we tried multiple



lengths and stopped at the first one that is not overfitting on the data inside the window (the same procedure is repeated for all the baselines).

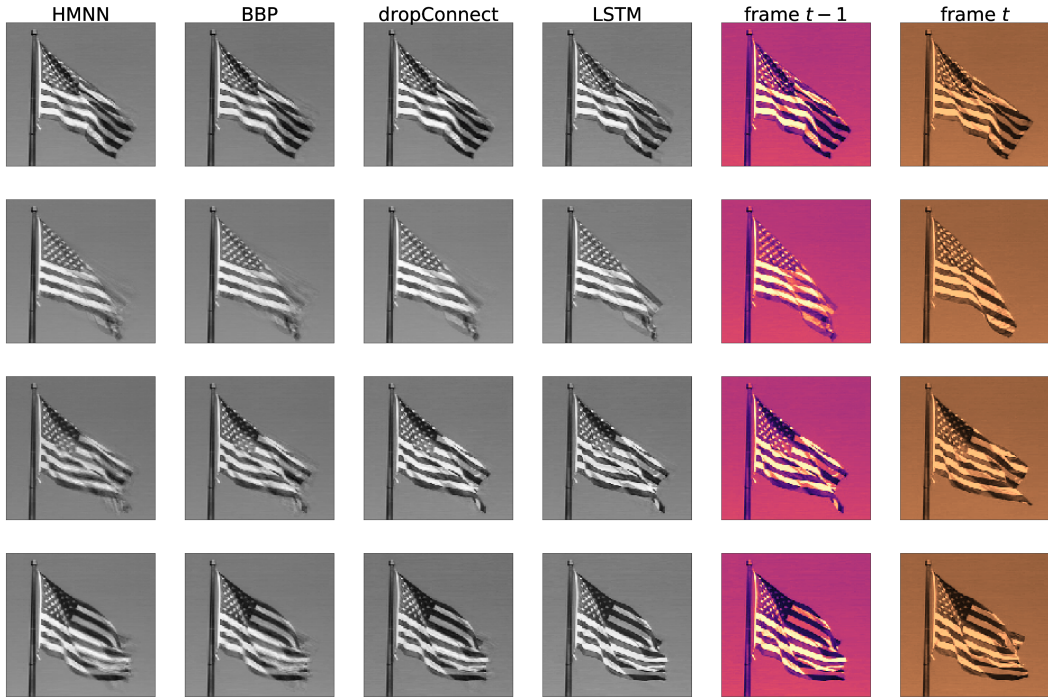


**Figure 8:** Columns show the prediction for different algorithms, with the last two being the last frame seen and the target frame. Rows display different time steps.

**Table 4:** Metric  $\mathcal{M}$  value on the test set (the smaller is the better).

Model	$\mathcal{M}$
Trivial Predictor	0.2162
LSTM	0.2080
DropConnect	0.2063
BBP	0.1932
HMNN	0.1891

Per each time step, we use a simple architecture of three layers with 500, 20, 500 rectified linear units, the vectorized previous frame as input and the vectorized current frame as output (the dimension is reduced with PCA). We consider fully Gaussian HMNN, with  $\mu = m_{t-1}$

(kernel parameter) and all the other parameters selected through random grid search and validation. Figure 8 compares HMNN predictions with different baselines: Bayes by Backprop trained sequentially on the sliding windows (column named BBP), DropConnect trained sequentially on the sliding windows (column named DropConnect), LSTM trained with the same sliding window size (column named LSTM), a trivial predictor that uses the previous frame as forecasting for the current frame (column named: frame  $t-1$ ). We notice that LSTM is prone to overfit on the sliding window and so to predict frame  $t$  with the last frame seen without any uncertainty. Similar issues appear in sequential DropConnect. This unwanted behaviour is probably due to the absence of uncertainty quantification and so overconfidence in the considered predictions. HMNN and sequential BBP are less certain about prediction and they create blurred regions where they expect the image to change. This phenomenon is particularly evident in the last row of Figure 8. Table 4 summarizes the performances using metric (17). Overall, HMNN performs better than the baselines and it is directly followed by the sequential BBP.

## 5 Discussion

We introduce a novel hybrid model between the Bayesian neural network and FHMM called the Hidden Markov neural network (HMNN), where the posterior distribution over the weights is estimated sequentially through variational Bayes with an evolving prior distribution, that is obtained by propagating forward through a stochastic transition kernel the variational approximation at the previous time step on the same vein of assumed density filter [Sorenson and Stubberud \(1968\)](#); [Minka \(2001\)](#). We use a variational approximation that induces a regularization technique called variational DropConnect, which resembles DropConnect ([Wan et al., 2013](#)) and variational DropOut ([Kingma et al., 2015](#)) and we reformulate the reparameterization trick according to it. We test variational DropConnect on MNIST. We analyse the behaviour of HMNNs in a simple conceptual drift framework. We compare HMNN with multiple baselines in a complex conceptual drift scenario and in time-series prediction. In all the experiments our method compares favourably against the considered baselines.

The idea behind HMNN is simple and it opens multiple research questions that can be answered in future works. Firstly the quality of the approximation is not treated and we are not even sure about the rate of accumulation of the error over time. Theoretical studies on variational approximations could be used to answer this matter ([Yang et al., 2017](#); [Chérif-Abdellatif, 2019](#)). Secondly, we do not propose any smoothing algorithm, which could improve the performance of HMNN and could open the avenue for an EM estimation of the hyperparameters, which could also be estimated by approximating the likelihood via sampling from the variational approximation. Thirdly, we have limited our studies to neural networks with simple architecture, it is surely possible to use similar techniques in recurrent neural networks and convolutional neural networks, to tackle more complicated applications. Finally, the variational DropConnect can be applied in multiple variational Bayes scenarios to check if it leads to better performances.

## References

- Aitchison, L. (2018). Bayesian filtering unifies adaptive and non-adaptive neural network optimization methods. *arXiv preprint arXiv:1807.07540*.
- Aitchison, L., A. Pouget, and P. E. Latham (2014). Probabilistic synapses. *arXiv preprint arXiv:1410.1029*.
- Basharat, A. and M. Shah (2009). Time series prediction by chaotic modeling of nonlinear dynamical systems. In *2009 IEEE 12th international conference on computer vision*, pp. 1941–1948. IEEE.
- Bengio, Y., R. Cardin, R. De Mori, and Y. Normandin (1990). A hybrid coder for hidden markov models using a recurrent neural networks. In *International Conference on Acoustics, Speech, and Signal Processing*, pp. 537–540. IEEE.
- Bengio, Y., R. De Mori, G. Flammia, and R. Kompe (1991). Global optimization of a neural network-hidden markov model hybrid. In *IJCNN-91-Seattle International Joint Conference on Neural Networks*, Volume 2, pp. 789–794. IEEE.
- Blei, D. M., A. Kucukelbir, and J. D. McAuliffe (2017). Variational inference: A review for statisticians. *Journal of the American statistical Association* 112(518), 859–877.
- Blundell, C., J. Cornebise, K. Kavukcuoglu, and D. Wierstra (2015). Weight uncertainty in neural network. In *International Conference on Machine Learning*, pp. 1613–1622. PMLR.
- Boots, B., G. J. Gordon, and S. M. Siddiqi (2008). A constraint generation approach to learning stable linear dynamical systems. In *Advances in neural information processing systems*, pp. 1329–1336.
- Chan, A. B. and N. Vasconcelos (2007). Classifying video with kernel dynamic textures. In *2007 IEEE Conference on Computer Vision and Pattern Recognition*, pp. 1–6. IEEE.
- Chopin, N. and O. Papaspiliopoulos (2020). *Introduction to Sequential Monte Carlo*. Springer International Publishing.
- Chérif-Abdellatif, B.-E. (2019). Convergence rates of variational inference in sparse deep learning.
- Feldkamp, L. A., D. V. Prokhorov, and T. M. Feldkamp (2003). Simple and conditioned adaptive behavior from kalman filter trained recurrent networks. *Neural Networks* 16(5-6), 683–689.
- Franzini, M., K.-F. Lee, and A. Waibel (1990). Connectionist viterbi training: a new hybrid method for continuous speech recognition. In *International Conference on Acoustics, Speech, and Signal Processing*, pp. 425–428. IEEE.
- Gal, Y. and Z. Ghahramani (2016). Dropout as a bayesian approximation: Representing model uncertainty in deep learning. In *international conference on machine learning*, pp. 1050–1059.

- Ghahramani, Z. and M. I. Jordan (1997, Nov). Factorial hidden markov models. *Machine Learning* 29(2), 245–273.
- Glorot, X., A. Bordes, and Y. Bengio (2011). Deep sparse rectifier neural networks. In *Proceedings of the fourteenth international conference on artificial intelligence and statistics*, pp. 315–323.
- Graves, A. (2011). Practical variational inference for neural networks. In *Advances in neural information processing systems*, pp. 2348–2356.
- Johnson, M. J., D. Duvenaud, A. B. Wiltschko, S. R. Datta, and R. P. Adams (2016). Composing graphical models with neural networks for structured representations and fast inference. *arXiv preprint arXiv:1603.06277*.
- Karl, M., M. Soelch, J. Bayer, and P. Van der Smagt (2016). Deep variational bayes filters: Unsupervised learning of state space models from raw data. *arXiv preprint arXiv:1605.06432*.
- Kingma, D. P., T. Salimans, and M. Welling (2015). Variational dropout and the local reparameterization trick. In *Advances in neural information processing systems*, pp. 2575–2583.
- Kingma, D. P. and M. Welling (2013). Auto-encoding variational bayes, 2013. *URL* <https://arxiv.org/abs/1312.6114>.
- Kirkpatrick, J., R. Pascanu, N. Rabinowitz, J. Veness, G. Desjardins, A. A. Rusu, K. Milan, J. Quan, T. Ramalho, A. Grabska-Barwinska, et al. (2017). Overcoming catastrophic forgetting in neural networks. *Proceedings of the national academy of sciences* 114(13), 3521–3526.
- Krishnan, R., U. Shalit, and D. Sontag (2017). Structured inference networks for nonlinear state space models. In *Proceedings of the AAAI Conference on Artificial Intelligence*, Volume 31.
- Krogh, A., B. Larsson, G. Von Heijne, and E. L. Sonnhammer (2001). Predicting transmembrane protein topology with a hidden markov model: application to complete genomes. *Journal of molecular biology* 305(3), 567–580.
- Krogh, A. and S. K. Riis (1999). Hidden neural networks. *Neural Computation* 11(2), 541–563.
- Kurle, R., B. Cseke, A. Klushyn, P. van der Smagt, and S. Günnemann (2019). Continual learning with bayesian neural networks for non-stationary data. In *International Conference on Learning Representations*.
- LeCun, Y., L. Bottou, Y. Bengio, P. Haffner, et al. (1998). Gradient-based learning applied to document recognition. *Proceedings of the IEEE* 86(11), 2278–2324.
- Liu, L., X. Jiang, F. Zheng, H. Chen, G.-J. Qi, H. Huang, and L. Shao (2023). A bayesian federated learning framework with online laplace approximation. *IEEE Transactions on Pattern Analysis and Machine Intelligence*.

- Minka, T. P. (2001). *A family of algorithms for approximate Bayesian inference*. Ph. D. thesis, Massachusetts Institute of Technology.
- Mobiny, A., H. V. Nguyen, S. Moulik, N. Garg, and C. C. Wu (2019). Dropconnect is effective in modeling uncertainty of bayesian deep networks. *arXiv preprint arXiv:1906.04569*.
- Mobiny, A., P. Yuan, S. K. Moulik, N. Garg, C. C. Wu, and H. Van Nguyen (2021). Dropconnect is effective in modeling uncertainty of bayesian deep networks. *Scientific reports* 11(1), 5458.
- Nair, V. and G. E. Hinton (2010). Rectified linear units improve restricted boltzmann machines. In *Proceedings of the 27th international conference on machine learning (ICML-10)*, pp. 807–814.
- Nguyen, C. V., Y. Li, T. D. Bui, and R. E. Turner (2017). Variational continual learning. *arXiv preprint arXiv:1710.10628*.
- Ollivier, Y. et al. (2018). Online natural gradient as a kalman filter. *Electronic Journal of Statistics* 12(2), 2930–2961.
- Pedregosa, F., G. Varoquaux, A. Gramfort, V. Michel, B. Thirion, O. Grisel, M. Blondel, P. Prettenhofer, R. Weiss, V. Dubourg, et al. (2011). Scikit-learn: Machine learning in python. *Journal of machine learning research* 12(Oct), 2825–2830.
- Puskorius, G. V. and L. A. Feldkamp (1991). Decoupled extended kalman filter training of feedforward layered networks. In *IJCNN-91-Seattle International Joint Conference on Neural Networks*, Volume 1, pp. 771–777. IEEE.
- Puskorius, G. V. and L. A. Feldkamp (1994). Neurocontrol of nonlinear dynamical systems with kalman filter trained recurrent networks. *IEEE Transactions on neural networks* 5(2), 279–297.
- Puskorius, G. V. and L. A. Feldkamp (2001). Parameter-based kalman filter training: Theory and implementation. *Kalman filtering and neural networks*, 23.
- Rabiner, L. R. and B.-H. Juang (1986). An introduction to hidden markov models. *ieee assp magazine* 3(1), 4–16.
- Rebeschini, P., R. Van Handel, et al. (2015). Can local particle filters beat the curse of dimensionality? *The Annals of Applied Probability* 25(5), 2809–2866.
- Ritter, H., A. Botev, and D. Barber (2018). Online structured laplace approximations for overcoming catastrophic forgetting. In *Advances in Neural Information Processing Systems*, pp. 3738–3748.
- Salehin, I. and D.-K. Kang (2023). A review on dropout regularization approaches for deep neural networks within the scholarly domain. *Electronics* 12(14), 3106.

- Shah, S., F. Palmieri, and M. Datum (1992). Optimal filtering algorithms for fast learning in feedforward neural networks. *Neural networks* 5(5), 779–787.
- Sorenson, H. W. and A. R. Stubberud (1968). Non-linear filtering by approximation of the a posteriori density. *International Journal of Control* 8(1), 33–51.
- Srivastava, N., G. Hinton, A. Krizhevsky, I. Sutskever, and R. Salakhutdinov (2014). Dropout: a simple way to prevent neural networks from overfitting. *The journal of machine learning research* 15(1), 1929–1958.
- Venkatraman, A., M. Hebert, and J. A. Bagnell (2015). Improving multi-step prediction of learned time series models. In *Twenty-Ninth AAAI Conference on Artificial Intelligence*.
- Wan, L., M. Zeiler, S. Zhang, Y. Le Cun, and R. Fergus (2013). Regularization of neural networks using dropconnect. In *International conference on machine learning*, pp. 1058–1066.
- Wang, L., X. Zhang, H. Su, and J. Zhu (2024). A comprehensive survey of continual learning: theory, method and application. *IEEE Transactions on Pattern Analysis and Machine Intelligence*.
- Yang, Y., D. Pati, and A. Bhattacharya (2017).  $\alpha$ -variational inference with statistical guarantees. *arXiv preprint arXiv:1710.03266*.

## A Formulae derivation

The full derivation of the **KL**-divergence between the variational approximation and the evolving prior for a general time step  $t$  of an HMNN is:

$$\begin{aligned}
\mathbf{KL}(q_\theta || \mathbf{C}_t \mathbf{P} \pi_{t-1}) &:= \mathbb{E}_{q_\theta(w)} [\log(q_\theta(w)) - \log(\mathbf{C}_t \mathbf{P} \pi_{t-1}(w))] \\
&= \text{constant} + \mathbb{E}_{q_\theta(w)} [\log(q_\theta(w)) - \log(g(w, \mathcal{D}_t)) - \log(\mathbf{P} \pi_{t-1}(w))] \quad (18) \\
&= \text{constant} + \mathbf{KL}(q_\theta || \mathbf{P} \pi_{t-1}) - \mathbb{E}_{q_\theta(w)} [\log(g(w, \mathcal{D}_t))],
\end{aligned}$$

where:

$$\begin{aligned}
\log \mathbf{C}_t \mathbf{P} \pi_{t-1}(w) &= \log \left( \frac{g(w, \mathcal{D}_t) \mathbf{P} \pi_{t-1}(w)}{\int g(w, \mathcal{D}_t) \mathbf{P} \pi_{t-1}(w) dw} \right) \\
&= \log(g(w, \mathcal{D}_t)) + \log(\mathbf{P} \pi_{t-1}(w)) - \log \left( \int g(w, \mathcal{D}_t) \mathbf{P} \pi_{t-1}(w) dw \right). \quad (19)
\end{aligned}$$

The close form solution of  $\mathbf{P} \tilde{\pi}_{t-1}$  for a fully Gaussian HMNN is derived from the following

integral:

$$\begin{aligned}
(\mathbf{P}\tilde{\pi}_{t-1})^v(w^v) &= \int p(\tilde{w}^v, w^v)(\tilde{\pi}_{t-1})^v(\tilde{w}^v)d\tilde{w}^v \\
&= \gamma^v \phi \int \mathcal{N}(w^v | \mu^v + \alpha(\tilde{w}^v - \mu^v), \sigma^2) \mathcal{N}(\tilde{w}^v | m_{t-1}^v, (s_{t-1}^v)^2) d\tilde{w}^v \\
&\quad + (1 - \gamma^v) \phi \int \mathcal{N}(w^v | \mu^v + \alpha(\tilde{w}^v - \mu^v), \sigma^2) \mathcal{N}(\tilde{w}^v | 0, (s_{t-1}^v)^2) d\tilde{w}^v \\
&\quad + \gamma^v(1 - \phi) \int \mathcal{N}(w^v | \mu^v + \alpha(\tilde{w}^v - \mu^v), \sigma^2/c^2) \mathcal{N}(\tilde{w}^v | m_{t-1}^v, (s_{t-1}^v)^2) d\tilde{w}^v \\
&\quad + (1 - \gamma^v)(1 - \phi) \int \mathcal{N}(w^v | \mu^v + \alpha(\tilde{w}^v - \mu^v), \sigma^2/c^2) \mathcal{N}(\tilde{w}^v | 0, (s_{t-1}^v)^2) d\tilde{w}^v,
\end{aligned} \tag{20}$$

the formulation in the main paper can be achieved by applying the following lemma to each element of the sum in (20).

**Lemma 1.** Consider a Gaussian random variable  $W \sim \mathcal{N}(\cdot | \mu_1, \sigma_1^2)$  and let:

$$\tilde{W} = \mu_2 - \alpha(\mu_2 - W) + \sigma_2 \xi, \tag{21}$$

with  $\xi \sim \mathcal{N}(\cdot | 0, 1)$ . Then the distribution of  $\tilde{W}$  is again Gaussian:

$$\tilde{W} \sim \mathcal{N}(\cdot | \mu_2 - \alpha(\mu_2 - \mu_1), \sigma_2^2 + \alpha^2 \sigma_1^2). \tag{22}$$

*Proof.* Note that the distribution  $p(\tilde{w}|w)$  of  $\tilde{W}|W$  is a Gaussian distribution, so  $p(\tilde{w}) = \int p(\tilde{w}|w)p(w)dw$  is an integral of the same form of the ones in (20). The distribution of  $\tilde{W}$  can be directly computed by noting that  $\tilde{W}$  is a linear combination of two independent Gaussians and a scalar, and consequently, it is Gaussian itself. The lemma is proved by computing the straightforward mean and variance from formulation (21).  $\square$

## B Experiments

This section presents a subsection for each experiment:

- subsection B.1 treats the experiment on Variational DropConnect;
- subsection B.3 describes the application to the evolving classifier;
- subsection B.4 considers the video texture of a waving flag.

Unless we specify differently, we train using vanilla gradient descent with learning rate  $\gamma$ .

### B.1 Variational DropConnect: supplementary material

We train on the MNIST dataset consisting of 60000 images of handwritten digits with sizes 28 by 28. The images are preprocessed by dividing each pixel by 126. We use 50000 images for training and 10000 for validation. The test set is composed of 10000 images. Both training and test can be downloaded from “<http://yann.lecun.com/exdb/mnist/>” .

As for [Blundell et al. \(2015\)](#) we focus on an ordinary feed-forward neural network without any convolutional layers. We consider a small architecture with the vectorized image as input, two hidden layers with 400 rectified linear units ([Nair and Hinton, 2010](#); [Glorot et al., 2011](#)) and a softmax layer on 10 classes as output. We consider a cross-entropy loss and a fully Gaussian HMNN with a single time step. The Variational Dropconnect technique is applied only to the internal linear layers of the network, i.e. we are excluding the initial layer and the final one as in [LeCun et al. \(1998\)](#). Observe that a single time step HMNN with  $\gamma^v = 1, \alpha = 0$  and  $\mu = \mathbf{0}$  (vector of zeros) is equivalent to Bayes by Backprop. For this reason, we can simply use our implementation of HMNN to include Bayes by Backprop. We set  $T = 1, \alpha = 0, \mu = \mathbf{0}$  and we consider  $\gamma^v \in \{0.25, 0.5, 0.75, 1\}$ ,  $\phi \in \{0.25, 0.5, 0.75\}$ ,  $-\log(\sigma) \in \{0, 1, 2\}$ ,  $-\log(c) \in \{6, 7, 8\}$ , learning rate  $l \in \{10^{-5}, 10^{-4}, 10^{-3}\}$ .

We generate more than 50 random combinations of the parameters  $(p, \phi, \sigma, c, \gamma)$ , for each combination, we also randomly set the number of Monte Carlo simulations  $N \in \{1, 2, 5\}$ . We train each combination for 600 epochs and we consider a minibatch size of 128. We then choose the best three models per each possible value of  $p$  and we report the performance on the validation set in the main paper.

## B.2 Two moons dataset: supplementary material

We consider the following set of hyperparameters:  $\alpha = 0.5, \gamma^v = 0.75, \phi = 0.5, -\log(\sigma) = 2, \log(c) = 5, l = 10^{-3}$ .

## B.3 Evolving classifier on MNIST: supplementary material

The main feature of HMNN is the time dimension, hence we need an example where the data evolves in time. We decided to build this example from the MNIST dataset by simply changing the way in which we assign the labels.

1. We preprocess the data by dividing each pixel by 126. We then define two labellers:  $\mathcal{C}_1$ , naming each digit with its label in MNIST;  $\mathcal{C}_2$ , labelling each digit with its MNIST's label shifted by one unit, i.e. 0 is classified as 1, 1 is classified as 2,  $\dots$ , 9 is classified as 0.
2. We consider 19 time steps where each time step  $t$  is associated with a probability  $f_t \in [0, 1]$  and a portion of the MNIST's dataset  $\mathcal{D}_t$ . The probability of choosing  $\mathcal{C}_1$  evolves as follows:

$$f_t = \frac{1}{2} \sin \left( \frac{\pi}{8} \left( \frac{4t}{5} + \frac{16}{5} \right) \right) + \frac{1}{2}, \quad t = 1, \dots, 19,$$

here  $\pi$  is the actual Pi, i.e.  $\pi \approx 3.14$ .

3. At each time step  $t$  we randomly label each digit in  $\mathcal{D}_t$  with either  $\mathcal{C}_1$  or  $\mathcal{C}_2$  according to the probabilities  $f_t, 1 - f_t$ .

The above procedure is used for both training, validation and test sets. The sample size of each time step is 10000 for training and 5000 for validation and testing (we resample from the training set of MNIST to reach the desired sample size). To validate and test the models we



consider the mean classification accuracy over time:

$$\mathcal{A}(\mathcal{D}_{1:T}, \hat{\mathcal{D}}_{1:T}) := \frac{1}{T} \sum_{t=1}^T \frac{1}{|\mathcal{D}_t|} \sum_{x,y \in \mathcal{D}_t} \mathbb{I}_y(\hat{y}(x)), \quad (23)$$

where  $\mathcal{D}_t$  is the generated dataset of images  $x$  and labels  $y$ ,  $\hat{\mathcal{D}}_t$  is the collection of images  $x$  and predictions  $\hat{y}(x)$  on the images  $x$  using the considered model,  $|\mathcal{D}_t|$  is the number of elements in  $\mathcal{D}_t$ , i.e. the total number of labels or images.

We consider a fully Gaussian HMNN with  $\mu = m_{t-1}$ , to encourage a strong memory on the previous posterior. The evolving in-time NN is composed of the vectorized image as input, two hidden layers with 100 rectified linear units and a softmax layer on 10 classes as output, and we consider a cross-entropy loss function. The Variational DropConnect technique is again applied to the internal linear layers of the network only. The parameters  $\alpha \in \{0.25, 0.5, 0.75, 1\}$  and  $\gamma^v \in \{0.25, 0.5, 0.75, 1\}$  are selected through the validation set (using metric (23)) while the other parameters are:  $\phi = 0.5$ ,  $-\log(\sigma) = 2$ ,  $-\log(c) = 4$ ,  $l = 10^{-3}$ ,  $N = 1$ . We also tried other values for  $\phi, \sigma, c, l, N$  but we did not experience significant changes in terms of performance. We try all the possible combinations of  $\alpha, l$  and we train on the generated training set for 19 time steps and 100 epochs per each  $\mathcal{D}_t$ . Remark that a single  $\mathcal{D}_t$  is a collection of images and labels and it can be seen as a whole dataset itself.

We compare our method with four algorithms. The architecture of the NN is the same as that of HMNN.

- Sequential Bayes by Backprop. At each time step  $t$  we train for 100 epochs on  $\mathcal{D}_t$ . The parameters are  $\phi = 0.5$ ,  $-\log(\sigma) = 2$ ,  $-\log(c) = 4$ ,  $l = 10^{-3}$ ,  $N = 1$ . The Bayesian NN at time  $t$  is initialized with the previous estimates  $m_{t-1}, s_{t-1}$ .
- Bayes by Backprop on the whole dataset. We train for 100 epochs on the whole dataset (no time dimension, the sample size is 190000) a Bayesian NN with Bayes by Backprop. The parameters are  $\phi = 0.5$ ,  $-\log(\sigma) = 2$ ,  $-\log(c) = 4$ ,  $l = 10^{-3}$ ,  $N = 1$ .
- Elastic Weight Consolidation. At each time step  $t$  we train for 100 epochs on  $\mathcal{D}_t$ . The tuning parameter is chosen from the grid  $\{10, 100, 1000, 10000\}$  through the validation set and the metric (23). We find out that ADAM works better hence we train with it. Remark that this method is not Bayesian, but it is a well-known baseline for continual learning.
- Variational Continual Learning. At each time step  $t$  we train for 100 epochs on  $\mathcal{D}_t$ . We choose the learning rate from the grid  $\{10^{-3}, 10^{-4}, 10^{-5}\}$  through validation and the metric (23). The training is pursued without the use of a coreset because we are not comparing rehearsal methods.

Sequential classification accuracies on the validation set and test performances using (23) are shown in the main paper.

## B.4 One-step-ahead prediction for flag waving: supplementary material

A video has an intrinsic dynamic given by the sequence of frames, which makes HMNN suitable for a one-step-ahead prediction video’s frame. Here we consider the video of a waving flag.

The preprocessing phase is similar to MNIST: the video is converted into a sequence of frames in greyscale that are additionally divided by 126 and put in a vector form. We then reduce the dimension with PCA (130 principal components). We use 300 frames in total, validate on the frames from 100 to 150 and test on the last 150 frames. Note that we have a single video available, hence we need to perform validation and test online, meaning that validation and test sets are also part of the training, but they are not seen in advance. Precisely, during validation we train on the full path from 1 to 150, we make predictions on the frames from 100 to 150 using HMNN from time 99 to 149 and then we compute the associated metric on the considered path. Once the validation score is available, we perform model selection and continue the training on the next frames to get the performance on the test set. As explained in the main paper, we train sequentially on a sliding window that includes 36 frames.

Consider a fully Gaussian HMNN with a simple architecture of three layers with 500, 20, 500 rectified linear units, the vectorized previous frame as input and the vectorized current frame as output, and an MSE loss. We apply Variational DropConnect to all the linear layers. The parameters  $\alpha \in \{0.25, 0.5, 0.75\}$ ,  $\gamma^v \in \{0.3, 0.8, 1\}$ ,  $\phi = \{0.25, 0.5, 0.75\}$  are chosen according to the validation set. For the other parameters, we find that setting  $\log(\sigma) = 2, \log(c) = 8, l = 10^{-4}, N = 1$  performs the best. We train for 150 epochs on each sliding window

We compare with four models. The architectures for sequential Bayes by Backprop and sequential DropConnect are the same as HMNN. For implementation purposes, we consider an architecture of three layers with 500, 500, 500 rectified linear units for the LSTM.

- Sequential Bayes by Backprop. At each time step  $t$  we trained on the current sliding window for 150 epochs. The parameter  $\phi = \{0.25, 0.5, 0.75\}$  is chosen with grid search and  $\log(\sigma) = 2, \log(c) = 8, l = 10^{-4}, N = 1$ . We find that other choices of  $\sigma, c, l, N$  do not improve the performance. The Bayesian neural network at time  $t$  is initialized with the estimates at time  $t - 1$ .
- Sequential DropConnect. At each time step  $t$  we trained on the current sliding window for 150 epochs. The learning rate  $l = \{10^{-3}, 10^{-4}, 10^{-5}\}$  is chosen with grid search using the validation score. The neural network at time  $t$  is initialized with the estimates at time  $t - 1$ . This is not a Bayesian method.
- LSTM. We choose a window size of 36 and we choose the learning rate  $l = \{10^{-3}, 10^{-4}, 10^{-5}\}$  with grid search using the validation score. This is not a Bayesian method.
- Trivial predictor. We predict frame  $t$  with frame  $t - 1$ . We decided to include this trivial baseline because it is an indicator of overfitting on the current window.

Given that we extract 30 frames per second, successive frames look almost equal, this makes the comparison with the trivial predictor unfair. Testing on a subpath makes the metric  $\mathcal{M}$  more sensitive to big changes and it gives us a clearer measure of the learned patterns. Hence, we test on the subpath 150, 152, 154,  $\dots$  300 (we skip all the odd frames from 150 to 300). As already explained this is just a subset of the full test set and no algorithm is discarding any frames during training.